Automatic Segmentation of Anatomical Structures for Core Decompression Procedures

Student: Mingxu Liu (mliu90@jhu.edu)

Mentors: Ping-Cheng Ku (pku1@jhu.edu)

Alejandro Martin-Gomez (alejandro.martin@jhu.edu)

JOHNS HOPKINS
WHITING SCHOOL
of ENGINEERING

Project Overview

Osteonecrosis of the femoral head (ONFH)

- Osteonecrosis of the femoral head (ONFH): bone cells in the hip joint are dead due to insufficient blood supply to the femoral head[1].
- ONFH can lead to the collapse of the subchondral bone [1].

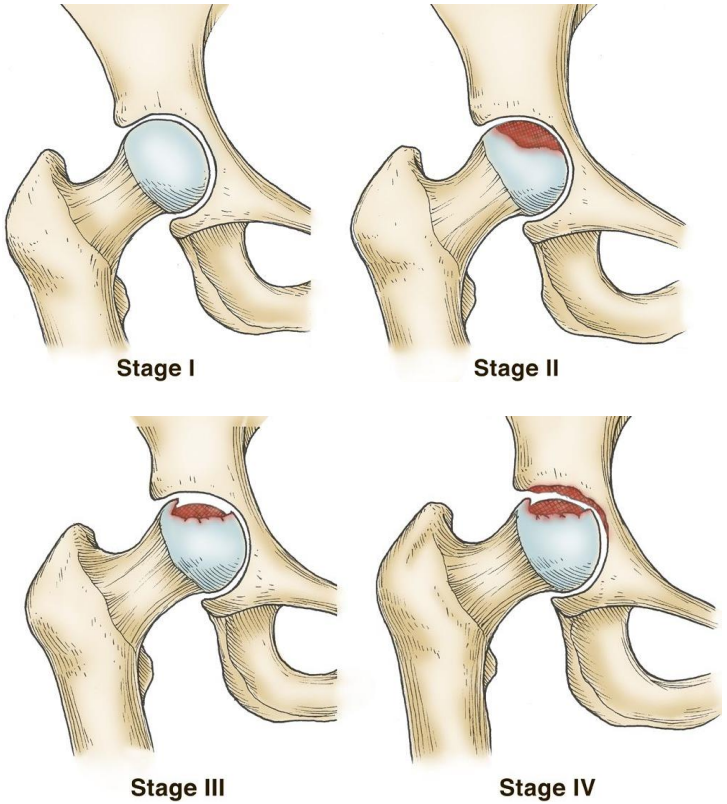

Image source: https://orthoinfo.aaos.org/en/diseases--conditions/osteonecrosis-of-the-hip

[1] Konstantinos N. Malizos, Apostolos H. Karantanas, Sokratis E. Varitimidis, Zoe H. Dailiana, Konstantinos Bargiotas, and Thomas Maris. Osteonecrosis of the femoral head: Etiology, imaging and treatment. European Journal ofRadiology, 63(1):16–28, 2007. Hip Joint.

Core Decompression

- Drill (multiple) holes in the femoral neck to access and remove the lesion [3].
- Reduces pressure, recover vascular inflow to the femoral head [3].
- Commonly used in the early stages of ONFH (Stage I and II) to prevent or delay the necessity for THA [4].

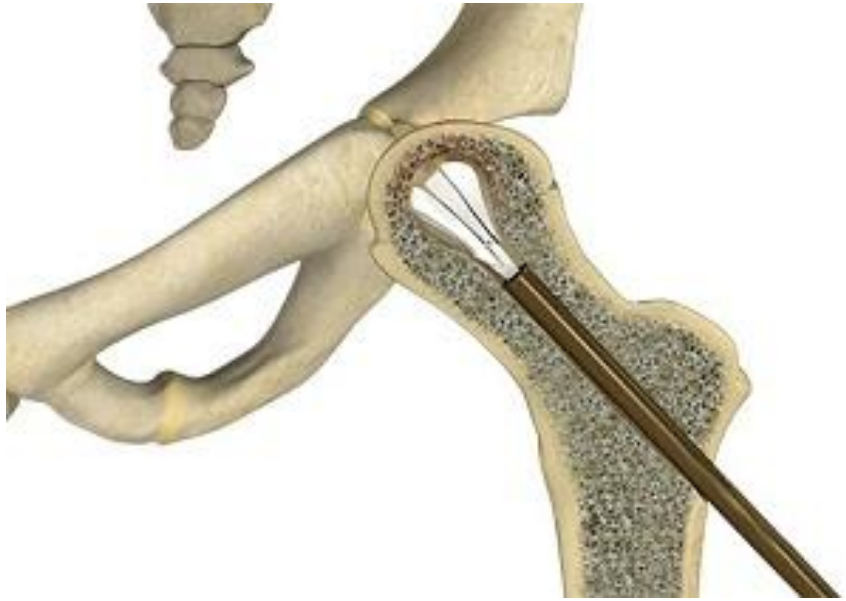

Image source: https://www.stlosm.com/core-decompression-avascular-necrosis-of-hip-orthopedics-sports-medicine-specialists-creve-coeur-missouri.html

[3]. Daniel Petek, Didier Hannouche, and Domizio Suva. Osteonecrosis of the femoral head: pathophysiology and current concepts of treatment. EFORT Open Reviews, 4(3):85 – 97, 2019.

[4]. Konstantinos N. Malizos, Apostolos H. Karantanas, Sokratis E. Varitimidis, Zoe H. Dailiana, Konstantinos Bargiotas, and Thomas Maris. Osteonecrosis of the femoral head: Etiology, imaging and treatment. European Journal of Radiology, 63(1):16–28, 2007. Hip Joint.

Pre-op and Intra-op Imaging

MRI (Pre-op)

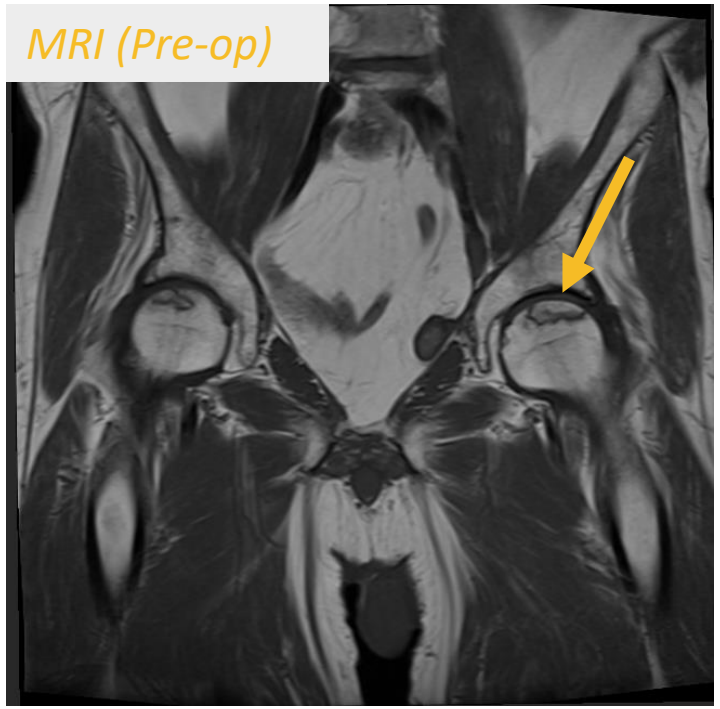

- Diagnosis
- Assessment of bone quality
- Surgical planning

CT (Intra-op)

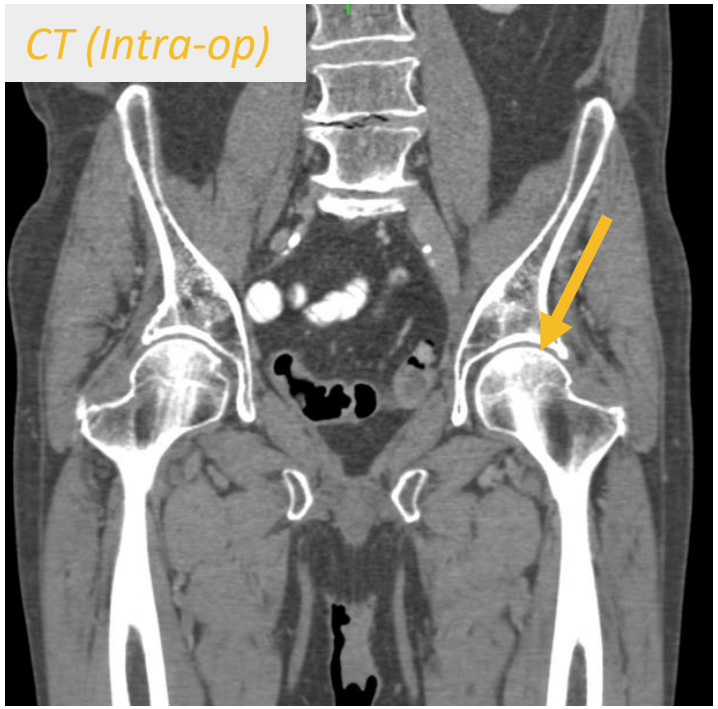

- Surgical Navigation

*Images provided by Alejandro Martin-Gomez

Registration between Pre-op and Intra-op Imaging

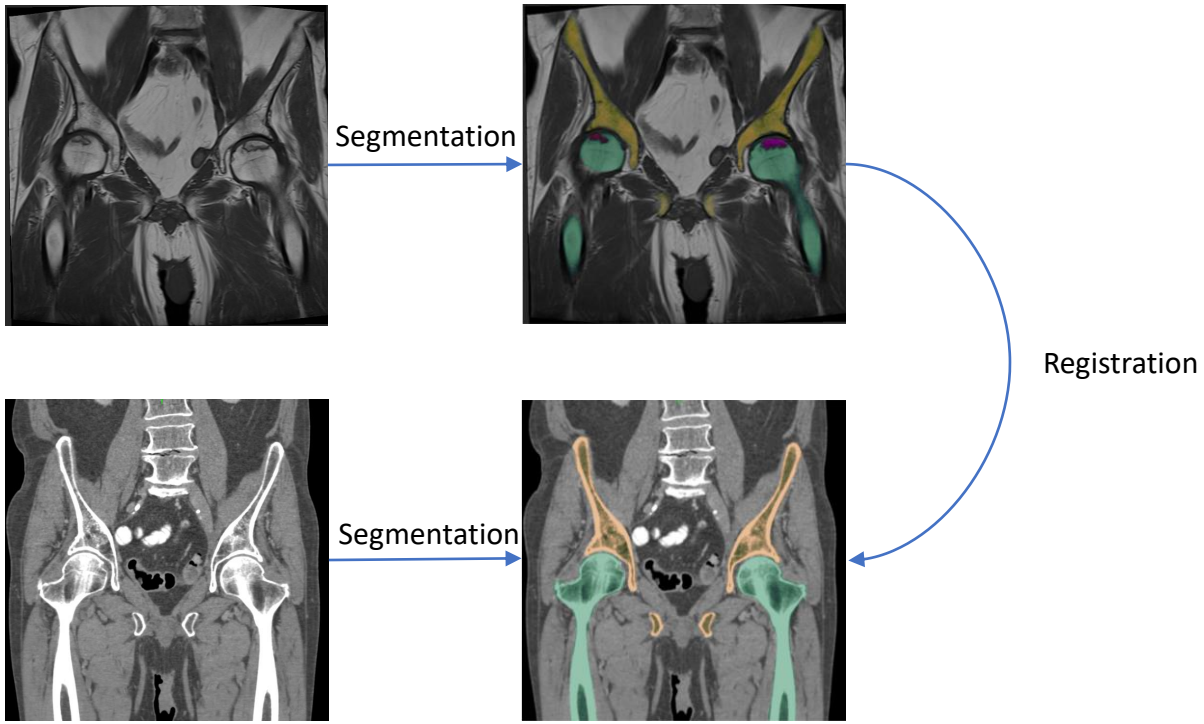

<u>Registration between MRI and CT is required.</u>

- Transform surgical plan from MRI to CT

Goal

- **Realize the automatic segmentation of the anatomical structures, including femur, pelvis, and necrosis, in MRI volumes used for the core decompression procedure.**
- **Realize the automatic segmentation of the femur and pelvis in CT volumes used for the core decompression procedure.**
- Realize the registration between the segmented anatomical structures (femur and pelvis) in MRI (first goal) and CT (second goal). A further topic is integrating the segmentation and registration models to form an integrated system and realize its interaction with 3D Slicer.

Paper I: Segmentation of the Proximal Femur from MR Images using Deep Convolutional Neural Networks.

www.nature.com/scientificreports

SCIENTIFIC REPORTS

OPEN

Segmentation of the Proximal Femur from MR Images using Deep Convolutional Neural Networks

Received: 12 March 2018
Accepted: 26 October 2018
Published online: 07 November 2018

Cem M. Deniz[1,2], Siyuan Xiang[3], R. Spencer Hallyburton[4], Arakua Welbeck[2], James S. Babb[2], Stephen Honig[5], Kyunghyun Cho[3,6] & Gregory Chang[1]

Magnetic resonance imaging (MRI) has been proposed as a complimentary method to measure bone quality and assess fracture risk. However, manual segmentation of MR images of bone is time-consuming, limiting the use of MRI measurements in the clinical practice. The purpose of this paper is to present an automatic proximal femur segmentation method that is based on deep convolutional neural networks (CNNs). This study had institutional review board approval and written informed consent was obtained from all subjects. A dataset of volumetric structural MR images of the proximal femur from 86 subjects were manually-segmented by an expert. We performed experiments by training two different CNN architectures with multiple number of initial feature maps, layers and dilation rates, and tested their segmentation performance against the gold standard of manual segmentations using four-fold cross-validation. Automatic segmentation of the proximal femur using CNNs achieved a high dice similarity score of 0.95 ± 0.02 with precision $= 0.95 \pm 0.02$, and recall $= 0.95 \pm 0.03$. The high segmentation accuracy provided by CNNs has the potential to help bring the use of structural MRI measurements of bone quality into clinical practice for management of osteoporosis.

Osteoporosis is a public health problem characterized by increased fracture risk secondary to low bone mass and microarchitectural deterioration of bone tissue. Hip fractures have the most serious consequences, requiring hospitalization and major surgery in almost all cases. Early diagnosis and treatment of osteoporosis play an important role in preventing osteoporotic fracture. Bone mass or bone mineral content is currently assessed most commonly via dual-energy x-ray absorptiometry (DXA)[1–3]. Over the years, cross-sectional imaging methods such as quantitative computed tomography (qCT)[4–9] and magnetic resonance imaging (MRI)[10–14] have been shown to provide useful additional clinical information beyond DXA secondary to their ability to image bone in 3-D and provide metrics of bone structure and quality[15].

MRI has been successfully performed *in vivo* for structural imaging of trabecular bone architecture within the proximal femur[16–18]. MRI provides direct detection of trabecular architecture by taking advantage of the MR signal difference between bone marrow and trabecular bone tissue itself. Osteoporosis related fracture risk assessment using MR images requires image analysis methods to extract information from trabecular bone using structural markers, such as topology and orientation of trabecular networks[19–21], or using finite element (FE) modeling[22–24]. Bone quality metrics derived from FE analysis of MR images are shown to correlate with high resolution qCT imaging, and may reveal different information about bone quality than that provided by DXA[18]. These technical developments overlay the significance of image analysis tools to determine osteoporosis related hip fracture risk.

Initial studies of MRI assessment of bone quality in proximal femur focused on quantification of parameters within specific regions of interest (ROI), such as the femoral neck, femoral head, and Ward's triangle, for extracting fracture risk relevant parameters[18]. More recently, investigation of the whole proximal femur has been proposed as a way to assess the mechanical properties or strength of the whole proximal femur, rather than just a subregion[25–27]. The latter, however, requires manual segmentation of the whole proximal femur[18,28] on MR

[1]Department of Radiology, New York University School of Medicine, New York, NY, 10016, USA. [2]Bernard and Irene Schwartz Center for Biomedical Imaging, New York University School of Medicine, New York, NY, 10016, USA. [3]Center for Data Science, New York University, New York, NY, 10012, USA. [4]Harvard College, Cambridge, MA, 02138, USA. [5]Osteoporosis Center, Hospital for Joint Diseases, New York University Langone Medical Center, New York, NY, 10003, USA. [6]Courant Institute of Mathematical Science, New York University, New York, NY, 10012, USA. Correspondence and requests for materials should be addressed to C.M.D. (email: cem.deniz@nyulangone.org)

Deniz, C.M., Xiang, S., Hallyburton, R.S. et al. Segmentation of the Proximal Femur from MR Images using Deep Convolutional Neural Networks. Sci Rep 8, 16485 (2018). https://doi.org/10.1038/s41598-018-34817-6

Paper I: Segmentation of the Proximal Femur from MR Images using Deep Convolutional Neural Networks.

Reason for selection:

- Segmentation networks specialized for femoral MRI images, highly relates to the main focus of the project
- Provides statistical conclusions on the performance of different architectures, which has reference significance for the selection of models.

Paper I: Segmentation of the Proximal Femur from MR Images using Deep Convolutional Neural Networks.

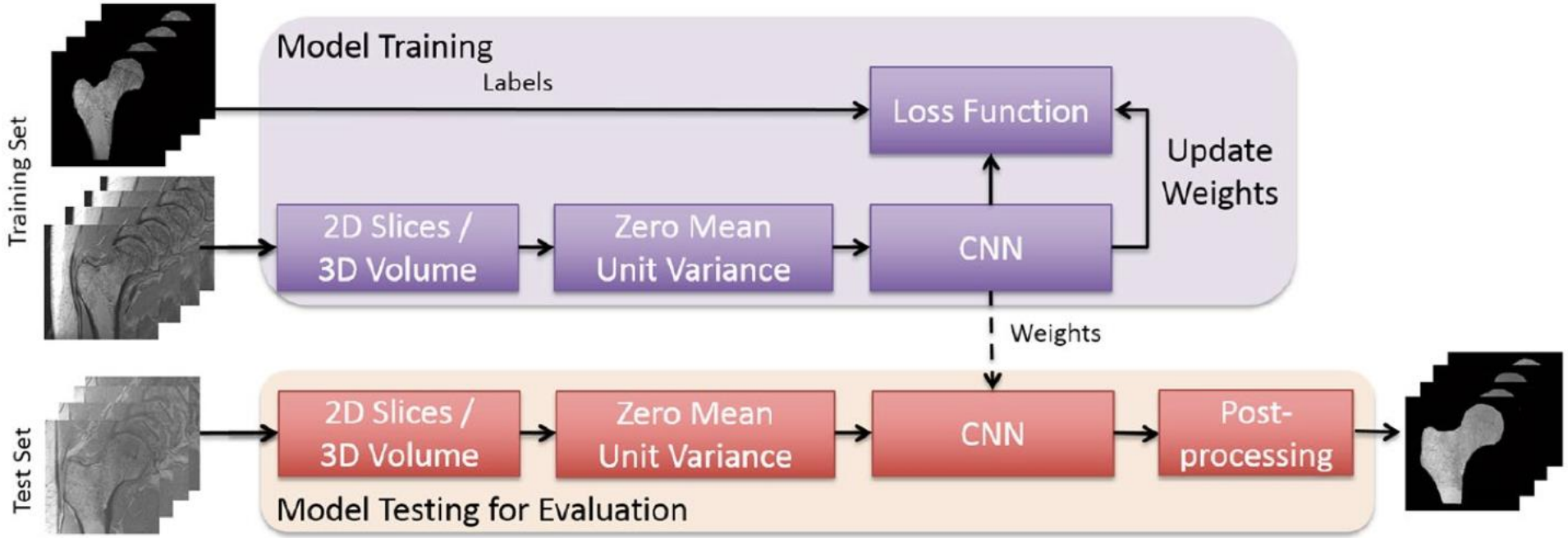

Figure 1. Overview of the proposed learning algorithm for an automatic segmentation of the proximal femur. Training CNN yields automatic proximal segmentation model that is used in model evaluation on a test dataset. The output of the model is the probability of the bone which is used to obtain the proximal femur segmentation mask using a threshold.

Paper I: Segmentation of the Proximal Femur from MR Images using Deep Convolutional Neural Networks.

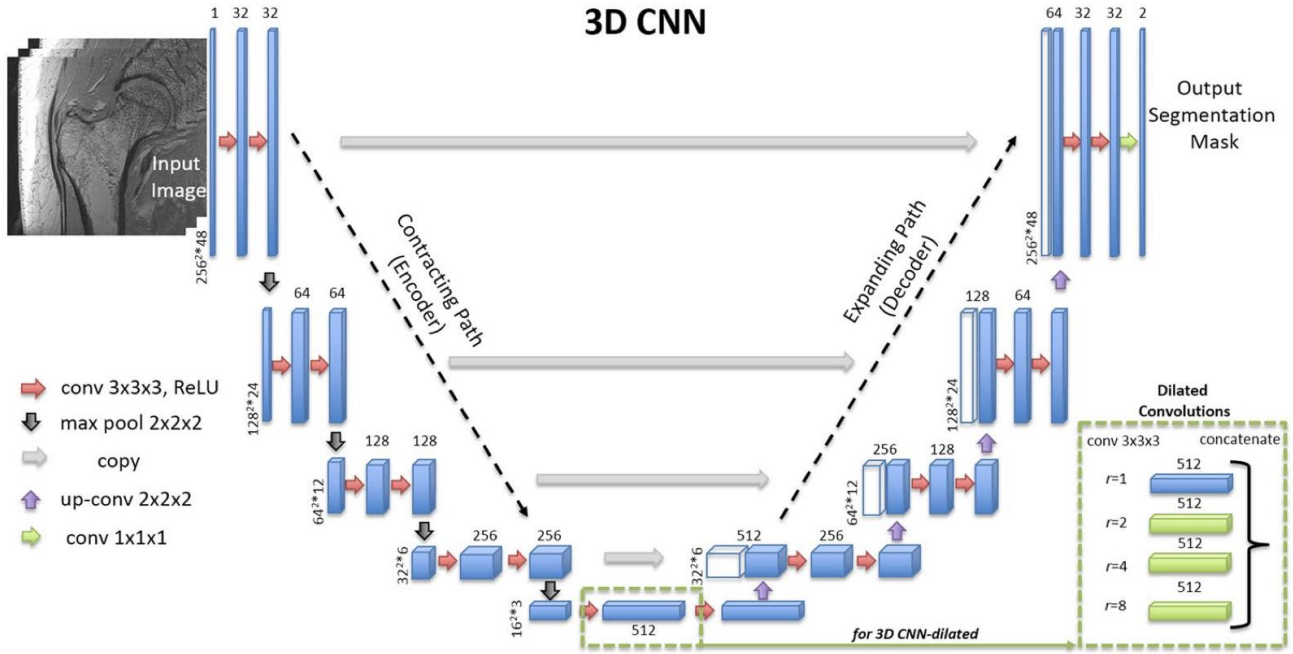

Figure 6. CNN architecture of one of the 3D CNNs used in the paper. Blue rectangles represent feature maps with the size and the number of feature maps indicated. Different operations in the network are depicted by color-coded arrows. The architecture represented here contains 32 feature maps in the first and last layer of the network and 4 layers in the contracting/expanding paths. In 3D CNN-dilated, dilated convolutions with multiple dilation rates are performed and concatenated (as indicated by green dashed boxes) at the center layer of the original 3D CNN.

- 2D U-Net, with three or four layers, initial feature map of 64 channels.
- 3D U-Net: with three or four layers, initial feature map of 16/32 channels.
- Dilated 2D/3D U-Net

Paper I: Segmentation of the Proximal Femur from MR Images using Deep Convolutional Neural Networks.

Experiments:

- conducted on 86 femur MRI volumes obtained from the New York University School of Medicine

- Four-fold cross validation with separation of 21/21/22/22

- Evaluated based on:

$$\text{D}ice\ Score(DSC) = 2TP/(FP + 2TP + FN)$$
$$\text{sensitivity/recall} = TP/(TP + FN)$$
$$\text{precision}\ (PPV) = TP/(TP + FP)$$

$$ASD = \frac{1}{N_S + N_G}\left(\sum_{x_S \epsilon S} d(x_S, G) + \sum_{x_G \epsilon G} d(x_G, S)\right)$$

$$MSD = \max\left\{\max_{x_S \epsilon S} d(x_S, G), \max_{x_G \epsilon G} d(x_G, S)\right\}$$

$$d(v, S) = \min_{s \in S} \|v - s\|$$

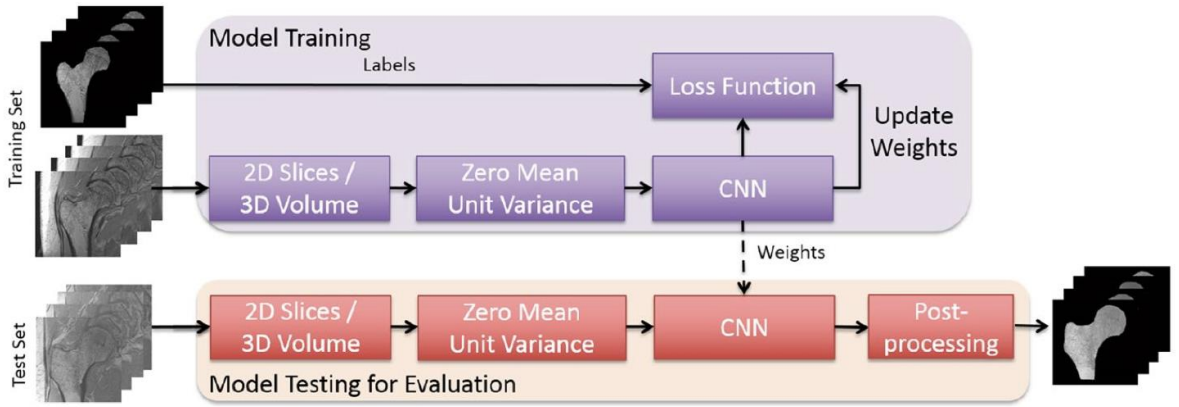

Paper I: Segmentation of the Proximal Femur from MR Images using Deep Convolutional Neural Networks.

Network	DSC ↑	Precision ↑	Recall ↑	ASD [mm] ↓	MSD [mm] ↓
2D CNN*, F:64, L:3	0.886 ± 0.055	0.890 ± 0.080	0.889 ± 0.056	6.15 ± 3.61	65.78 ± 5.78
2D CNN*, F:64, L:4	0.864 ± 0.044	0.872 ± 0.061	0.860 ± 0.060	6.82 ± 3.00	64.89 ± 6.36
2D CNN, F:64, L:3	0.924 ± 0.032	0.920 ± 0.041	0.930 ± 0.045	3.13 ± 1.76	54.40 ± 6.72
2D CNN, F:64, L:4	0.937 ± 0.026	0.932 ± 0.037	0.943 ± 0.036	2.13 ± 1.23	42.22 ± 5.52
2D CNN-dilated †, F:64, L:4	0.946 ± 0.022	0.948 ± 0.024	0.944 ± 0.034	1.75 ± 1.24	40.03 ± 8.37
3D CNN, F:16, L:3	0.927 ± 0.032	0.931 ± 0.029	0.927 ± 0.063	0.66 ± 0.32	10.62 ± 6.85
3D CNN, F:16, L:4	0.935 ± 0.028	0.938 ± 0.026	0.936 ± 0.053	0.59 ± 0.39	9.75 ± 6.56
3D CNN, F:32, L:3	0.942 ± 0.026	0.944 ± 0.022	0.942 ± 0.052	0.50 ± 0.25	11.97 ± 7.57
3D CNN, F:32, L:4	0.945 ± 0.029	0.948 ± 0.023	0.944 ± 0.052	0.45 ± 0.25	13.44 ± 13.14
3D CNN-dilated†, F:32, L:4	**0.953 ± 0.016**	**0.954 ± 0.017**	**0.953 ± 0.030**	**0.39 ± 0.20**	**7.88 ± 4.33**

Results and Main Conclusions:

- 3D U-Net outperforms than 2D U-Net

Paper I: Segmentation of the Proximal Femur from MR Images using Deep Convolutional Neural Networks.

Network	Dilation Rate (r)	AP ↑	DSC ↑	Precision ↑	Recall ↑	ASD [mm] ↓	MSD [mm] ↓
3D CNN F:32, L:4	1†	0.986 (0.002)	0.945 ± 0.029	0.948 ± 0.023	0.944 ± 0.052	0.45 ± 0.25	13.44 ± 13.14
	1, 2	0.988 (0.001)	0.950 ± 0.020	0.951 ± 0.017	0.949 ± 0.039	0.43 ± 0.23	8.77 ± 6.32
	1, 4	0.988 (0.002)	0.949 ± 0.019	0.948 ± 0.022	0.950 ± 0.036	0.43 ± 0.21	8.10 ± 4.73
	1, 8	0.988 (0.003)	0.948 ± 0.015	0.949 ± 0.023	0.948 ± 0.031	0.44 ± 0.19	8.05 ± 4.25
	1, 2, 4	0.988 (0.002)	0.948 ± 0.023	0.948 ± 0.021	0.949 ± 0.039	0.43 ± 0.24	8.14 ± 5.68
	1, 2, 4, 8	**0.992 (0.002)**	**0.953 ± 0.016**	**0.954 ± 0.017**	**0.953 ± 0.030**	**0.39 ± 0.19**	**7.88 ± 4.33**
2D CNN F:64, L:4	1†	0.979 (0.003)	0.937 ± 0.026	0.932 ± 0.036	0.943 ± 0.036	2.13 ± 1.22	42.22 ± 5.49
	1, 2	0.978 (0.002)	0.939 ± 0.025	0.937 ± 0.034	0.944 ± 0.037	2.04 ± 1.33	40.10 ± 7.34
	1, 4	0.984 (0.000)	0.943 ± 0.022	0.944 ± 0.026	0.944 ± 0.035	1.85 ± 1.13	39.70 ± 7.38
	1, 8	0.984 (0.002)	0.941 ± 0.023	0.941 ± 0.030	0.943 ± 0.034	2.04 ± 1.31	42.41 ± 7.60
	1, 2, 4	0.984 (0.005)	0.941 ± 0.025	0.941 ± 0.033	0.942 ± 0.034	2.02 ± 1.39	40.27 ± 7.76
	1, 2, 4, 8	0.986 (0.002)	0.946 ± 0.022	0.948 ± 0.024	0.944 ± 0.034	1.75 ± 1.24	40.03 ± 8.37

Results and Main Conclusions:

- 3D U-Net outperforms than 2D U-Net
- With dilated design, the models' performance can be improved, but still 3D U-Net overperforms than 2D U-Net

Paper I: Segmentation of the Proximal Femur from MR Images using Deep Convolutional Neural Networks.

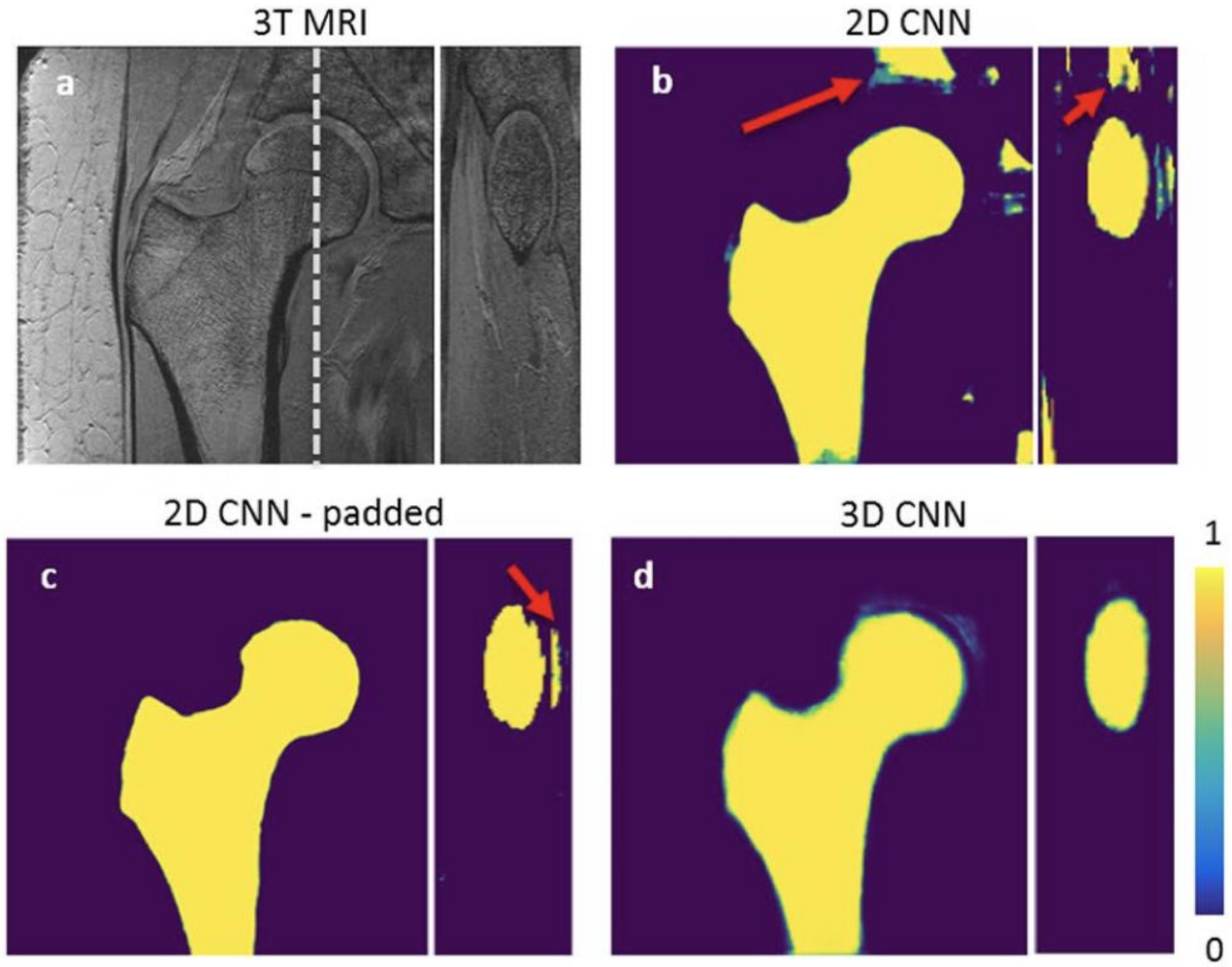

Results and Main Conclusions:

- 3D U-Net outperforms than 2D U-Net
- With dilated design, the models' performance can be improved, but still 3D U-Net overperforms than 2D U-Net
- 3D CNN performs better on segmentation accuracy on the hypointense regions, with fewer false positives.

Paper I: Segmentation of the Proximal Femur from MR Images using Deep Convolutional Neural Networks.

Pros:

- With considerable accuracy, greatly reduced the time for femur MRI segmentation, which has crucial implicational potential for the clinical diagnosis and treatment of osteonecrosis.
- Summarized the performance of various femur automatic segmentation models from five different evaluation metrics, which are contributive work and systemic guidance for similar tasks.

Cons:

- Use only the conventional convolutional layers, does not include more state-of-the-art U-Net variants, the performance of the model could be furtherly improved.

Paper II:
Fully Automatic and Fast Segmentation of the Femur Bone from 3D-CT Images with No Shape Prior

FULLY AUTOMATIC AND FAST SEGMENTATION OF THE FEMUR BONE FROM 3D-CT IMAGES WITH NO SHAPE PRIOR

Marcel Krčah[1,2] *Gábor Székely*[1] *Rémi Blanc*[1]

[1] Computer Vision Laboratory, ETH Zurich, Zurich, Switzerland
[2] Faculty of Mathematics and Physics, Charles University, Prague, Czech Republic

ABSTRACT

Statistical shape and intensity modelling have been subject to an increasing interest within the past decade. However, construction of such models requires large number of segmented examples. Accurate and automatic segmentation techniques that do not require any explicit prior model are therefore of high interest. We propose a fully-automatic method for segmenting the femur in 3D Computed Tomography (CT) volumes, based on graph-cuts and a bone boundary enhancement filter analysing the second-order local structure. The presented technique is evaluated in large-scale experiments, conducted on 197 femur samples, and compared to other three automatic bone segmentation methods. Our approach achieved accurate femur segmentation in 81% of cases without any shape prior or user interaction.

Index Terms— CT, bone segmentation, graph-cuts, sheetness measure, femur

1. INTRODUCTION

Statistical shape and intensity modeling have been subject to an increasing interest within the past decade in a wide variety of applications [1]. Particularly in the domain of orthopaedics, they are of high interest for intra-operative guidance, reconstructive surgery or implant design. However, learning such models requires that a large number of examples are available and pre-processed. Segmentation, in particular, remains a serious bottleneck in this context and manual processing is common practice. Accurate and automatic segmentation methods requiring no explicit prior model are therefore of high interest.

Segmentation of long bones in CT images is a relatively simple task, due to high contrast between the thick, strongly attenuating cortical layer and the encasing low-intensity soft tissue. However, segmentation still remains a challenge in the joint epiphysis areas, where the cortical layer becomes much thinner and the contrast between the cancellous bone and soft tissues is less pronounced. Additionally, the inter-bone space becomes very narrow and partial volume effects result in very weak contrast in these regions (Fig. 1a).

As pointed out in [2], despite several years of active research, bone segmentation remains in several aspects an open problem. Intensity-based methods, such as (local) binary thresholding or region growing, tend to produce discontinuous contours and "leakages" to soft-tissues or adjacent bones. Active contour models, such as snakes or level-set methods [3], are sensitive to initialization and are of limited use in areas of low gradient. More recently, the graph-cut framework [4, 5] has shown to provide an elegant and efficient approach for segmentation. It was applied to bone segmentation, e.g. in [6], with promising results. We extend this approach to a fully 3D formulation. In particular, we propose new energy terms for the graph-cut which utilize the sheetness measure inspired by [7]. A post-processing step is also presented for the automatic separation of adjacent bones.

Details of the proposed method are given in Section 2. In Section 3, we evaluate the method on a database of 197 cases, for which both original CTs and manual segmentations were available, and compare it with three other automatic methods. Section 4 concludes the paper.

2. OVERVIEW OF THE GRAPH-CUT SEGMENTATION PROCEDURE

The proposed procedure, illustrated in Fig. 1, is based on Boykov and Jolly's graph-cut segmentation framework [5], briefly presented in Section 2.1. To segment all bone tissues in the input 3D CT volume $\mathcal{I} : \Omega \rightarrow R$, the graph-cut relying on the terms described in Sections 2.2 and 2.3 is employed.

The output of the graph-cut is a binary volume with all bone-voxels labelled, as depicted in Fig. 1d. Due to narrow inter-bone spacing, the procedure is often not sufficient to perfectly segment the femur as leakage to adjacent bones (pelvis, tibia and patella) may occur. Experiments have shown that in such cases adjacent bones are connected to the femur generally by only a few voxels. Individual bones are therefore identified in a post-processing step, described in Section 2.4, and the femur is determined as the largest connected component in the final volume.

This work is part of the Virtual Skeleton Database project, NCCR Co-Me (http://co-me.ch), funded by the Swiss National Science Foundation.

978-1-4244-4128-0/11/$25.00 ©2011 IEEE 2087 ISBI 2011

Krcah, Marcel et al. "Fully automatic and fast segmentation of the femur bone from 3D-CT images with no shape prior." 2011 IEEE International Symposium on Biomedical Imaging: From Nano to Macro (2011): 2087-2090.

Paper II: Fully Automatic and Fast Segmentation of the Femur Bone from 3D-CT Images with No Shape Prior.

Reason for selection:

- Automatic CT segmentation of femur bone without given prior shape, highly related to the goal of the project. Also, has potential to be used for bone anatomies besides the femur --- could be used for pelvis segmentation as well.

Paper II: Fully Automatic and Fast Segmentation of the Femur Bone from 3D-CT Images with No Shape Prior.

Based on Graph-Cut Segmentation framework:

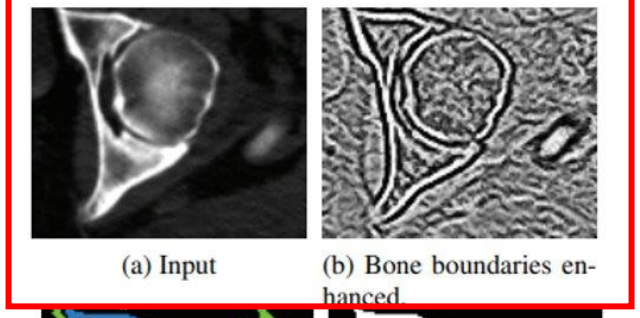

(a) Input (b) Bone boundaries enhanced

(c) Initialization of bone and background exclusion regions. (d) All bone voxels segmented.

(e) Bones identified with morphological erosion. (f) Final result

Boundary Enhancement using sheeting filter:

$$\mathcal{I}^U = \mathcal{I} + k(\mathcal{I} - \mathcal{I} \star G_s)$$

$$S_\sigma(x) = -\operatorname{sgn}(\lambda_3) \exp\left\{-\frac{R_{\text{sheet}}^2}{\alpha^2}\right\} \exp\left\{-\frac{R_{\text{tube}}^2}{\beta^2}\right\} \left(1 - \exp\left\{-\frac{R_{\text{noise}}^2}{\gamma^2}\right\}\right)$$

$$R_{\text{sheet}} = |\lambda_2|/|\lambda_3|$$

$$R_{\text{tube}} = |\lambda_1|/(|\lambda_2||\lambda_3|)$$

$$R_{\text{noise}} = (|\lambda_1| + |\lambda_2| + |\lambda_3|)/T$$

T: average trace o the Hessian at each image voxel

$\boldsymbol{\lambda_1}$, $\boldsymbol{\lambda_2}$ and $\boldsymbol{\lambda_3}$ are the eigenvalues of Hessian matrix and $|\boldsymbol{\lambda_1}| \leq |\boldsymbol{\lambda_2}| \leq |\boldsymbol{\lambda_3}|$.

Paper II: Fully Automatic and Fast Segmentation of the Femur Bone from 3D-CT Images with No Shape Prior.

Based on Graph-Cut Segmentation framework:

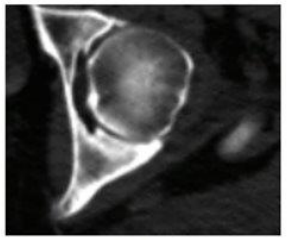

(a) Input

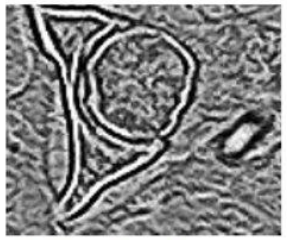

(b) Bone boundaries enhanced

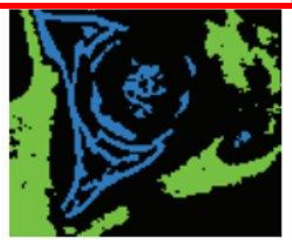

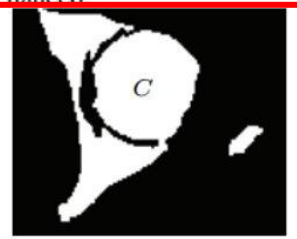

(c) Initialization of bone and background exclusion regions.

(d) All bone voxels segmented.

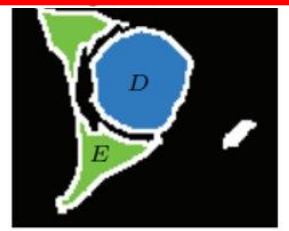

(e) Bones identified with morphological erosion.

(f) Final result

Segmentation by minimizing the energy function:

$$E(A) = \sum_{p \in \Omega} R_p(A_p) + \lambda \sum_{(p,q) \in \mathcal{N}} \delta(A_p, A_q) B(p,q)$$

$$B(p,q) \propto \begin{cases} \exp\left\{ -\frac{|S(p)-S(q)|}{\sigma_s} \right\} & \text{for } S(p) \geq S(q) \\ 1 & \text{otherwise} \end{cases}$$

$$R_p(A_p) \propto \begin{cases} 1 & \text{if } A_p = \text{"bone" and } p \in E_{\neg \text{ bone}} \\ 1 & \text{if } A_p = \text{"bkg" and } p \in E_{\neg bkg} \\ 0 & \text{otherwise.} \end{cases}$$

$$E_{\neg \text{ bkg}} = \{x \in \Omega \mid \mathcal{J}(x) \geq 400\text{HU} \wedge S(x) > 0\}$$
$$E_{\neg \text{ bone}} = \text{lcc}(\{x \in \Omega \mid \mathcal{J}(x) < -50\text{HU}\})$$

Paper II: Fully Automatic and Fast Segmentation of the Femur Bone from 3D-CT Images with No Shape Prior.

Based on Graph-Cut Segmentation framework:

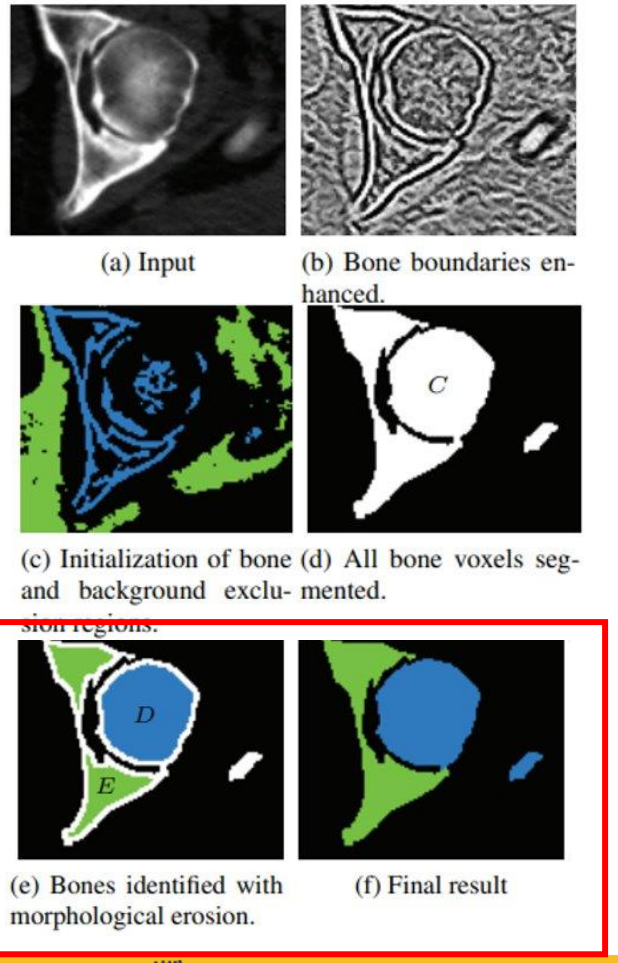

(a) Input (b) Bone boundaries enhanced.

(c) Initialization of bone and background exclusion regions. (d) All bone voxels segmented.

(e) Bones identified with morphological erosion. (f) Final result

Separate the bones, based on Graph-cut:

$$\forall p \in C : R_p(A_p) = \begin{cases} \infty & \text{if } A_p = \text{"D"} \text{ and } p \in E \\ \infty & \text{if } A_p = \text{"E"} \text{ and } p \in D \\ 0 & \text{otherwise.} \end{cases}$$

$$B(p,q) = B(q,p) = 1$$

Paper I: Segmentation of the Proximal Femur from MR Images using Deep Convolutional Neural Networks.

Experiments:

- 97 CT volumes which has been cropped around the femur are used for experiment.

- Evaluated based on:
  - True-Positive rate = $TP/(TP + FN)$
  - False-Positive rate = F$P/(TP + FN)$
  - Hausdorff distance between prediction and ground truth.

Paper II: Fully Automatic and Fast Segmentation of the Femur Bone from 3D-CT Images with No Shape Prior.

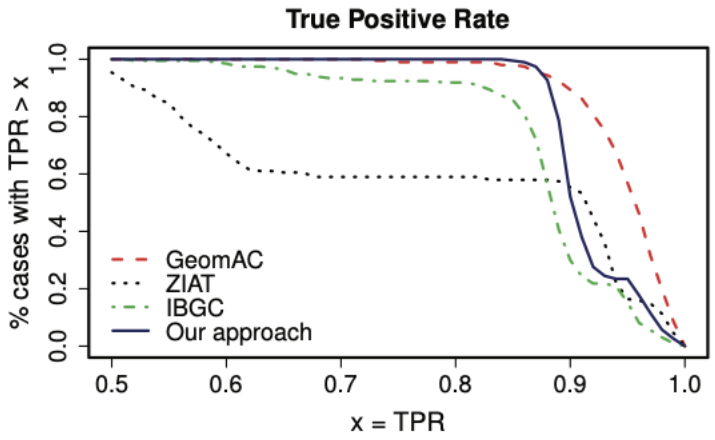

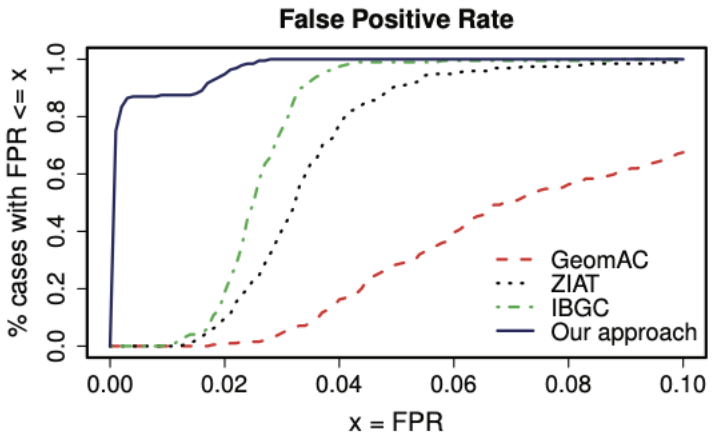

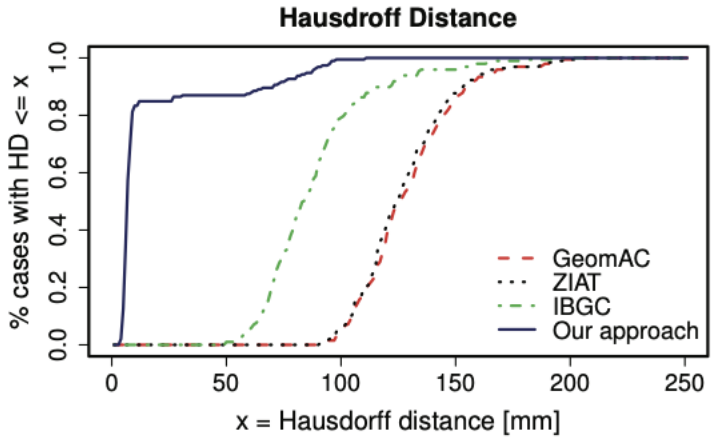

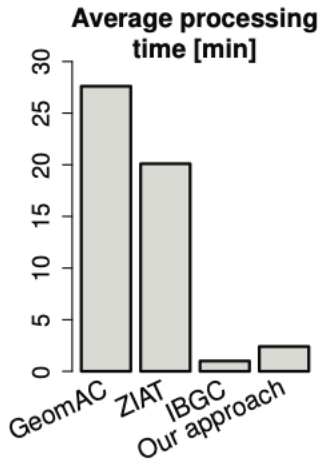

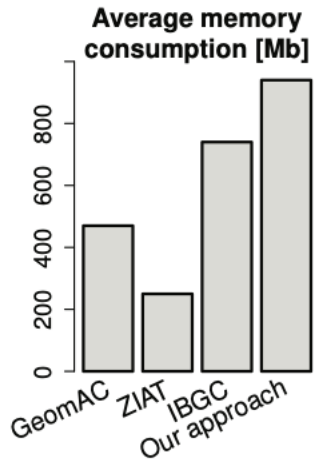

Results and Main Conclusions:

- True Positive rate > 0.85,
- False Positive rate < 0.001,
- Hausdorff Distance < 8mm in 81% of the tested cases.

Paper II: Fully Automatic and Fast Segmentation of the Femur Bone from 3D-CT Images with No Shape Prior.

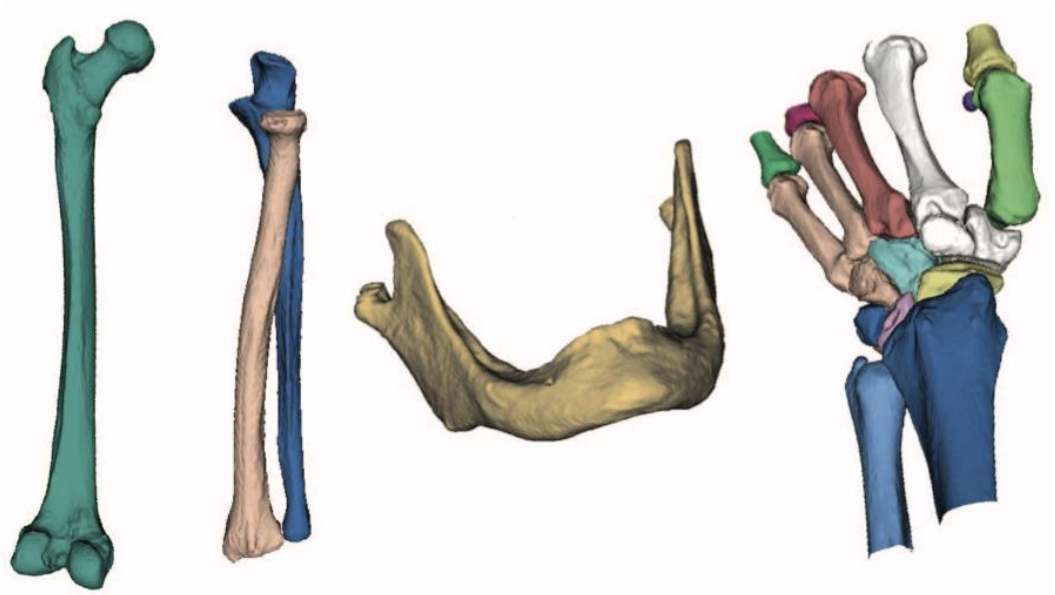

Fig. 4: 3D models generated from an automatically segmented femur, radius and ulna, mandible, carpal bones (from left to right).

Results and Main Conclusions:

Can be used for segmentation of different bone anatomies besides femur.

Paper II: Fully Automatic and Fast Segmentation of the Femur Bone from 3D-CT Images with No Shape Prior.

Pros:

- Using the graph-cut architecture and the thresholds based on the empirical data of CT segmentation, the algorithm can efficiently segment the CT bone structures. Algorithms outperform previous algorithms on multiple evaluation metrics.

Cons:

- Cannot distinguish between different bone anatomies.
- The performance of bone separation is not guaranteed.

Thank you!

Acknowledge

Thanks to Alejandro Martin-Gomez for providing the slides template